# DESIGN OF A MINIATURIZED DUAL-BAND ANTENNA FOR IMPROVED DIRECTIVITY USING A DIELECTRIC-LOADED CAVITY

**Maeng Chang Kang,[1] Gangil Byun,[2] and Hosung Choo[1]**
[1] School of Electronic and Electrical Engineering, Hongik University, Seoul, Korea; Corresponding author: kylebyun@gmail.com
[2] Research Institute of Science and Technology, Hongik University, Seoul, Korea

*Received 14 November 2015*

**ABSTRACT:** *This article proposes the design of a dual-band global positioning system (GPS) antenna using a high-permittivity dielectric-loaded cavity. The cavity structure is filled with a dielectric material to miniaturize the size, and its width and depth are adjusted to maximize the front-to-back ratio for high directivity. Dual-band circular polarization characteristics are achieved by placing two radiating polygon loops at the aperture of the cavity, and the loops are electromagnetically coupled to a microstrip line for a coupled feeding network. The proposed antenna is fabricated, and its antenna characteristics are measured in a full anechoic chamber. The results demonstrate that the antenna is suitable for dual-band GPS applications with high bore-sight gain values of 3.4 dBic at 1.2276 GHz and 3.7 dBic at 1.5754 GHz.*
 Microwave Opt Technol Lett 58:1591–1595, 2016; View this article online at wileyonlinelibrary.com. DOI 10.1002/mop.29854

**Key words:** *dual-band antenna; GPS antenna; microstrip antenna*

## 1. INTRODUCTION

Global positioning systems (GPSs) are widely used in various mobile system applications using signals received from GPS satellites located at an altitude of about 20,183 km. Thus, to compensate for the significant path loss with polarization mismatch in the ionosphere, these systems usually require high-gain antennas over the upper hemisphere with dual-band circular polarization (CP) characteristics [1]. To obtain high directivity in the upper hemisphere, there have been a lot of efforts made by adding a cavity structure at the bottom of the antennas, as presented in Refs. [2–8]. However, these studies were limited to either linear polarization or single-frequency operation, which is less suitable for GPS applications. Although a dual-band CP antenna using two resonating slots with an air-filled cavity structure was introduced in Ref. [9], it exhibits narrow matching and CP bandwidths because of its F-shaped feeding line. Furthermore, the air-filled cavity is insufficient to increase the directivity when the cavity area is restricted to a few square centimeters.

In this article, we propose the design of a dual-band CP antenna with a dielectric-loaded cavity to improve directivity in the upper hemisphere. The cavity structure is filled with a high dielectric material to miniaturize its size and is added at the bottom of the antenna to maximize the front-to-back ratio (FBR) in the bore-sight direction. For dual-band operation, two polygon loops are printed at the cavity aperture and are electromagnetically coupled to a microstrip feeding line. To verify the feasibility of the high-permittivity dielectric-loaded cavity, we fabricate the proposed antenna and measure its antenna characteristics in a full anechoic chamber. The results demonstrate that the proposed antenna structure is suitable for increasing the FBR with a miniaturized cavity size.

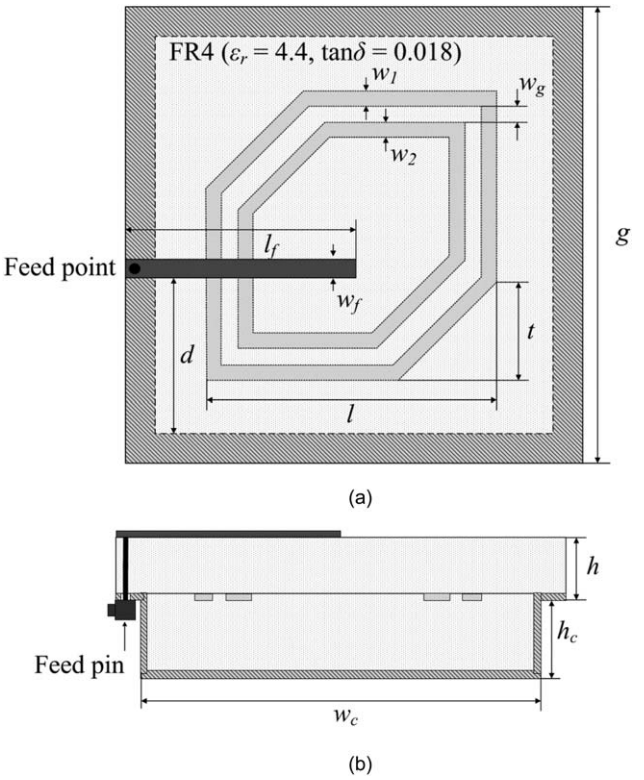


**Figure 1** Geometry of the proposed antenna. (a) Top view. (b) Side view

## 2. DESIGN APPROACH AND PROPOSED ANTENNA

Figure 1 shows the geometry of the proposed dual-band CP antenna structure with a dielectric-loaded cavity. The cavity structure is filled with a high dielectric material (FR4, $\varepsilon_r = 4.4$, $\tan\delta = 0.018$) to miniaturize the cavity dimension with improved FBR and CP properties. The cavity has a width of $w_c$ and a depth of $h_c$, and the depth is designed to be about a quarter guided wavelength ($\lambda_g$). Inner and outer polygon loops are designed to resonate in the GPS L1 and L2 bands, and their total lengths are determined to be approximately one wavelength ($\lambda_g$) using the parameters $l$, $t$, and $w_g$. The width of each loop, denoted as $w_1$ and $w_2$, is also an important parameter for impedance matching characteristics at each frequency band, and the parameter $t$ and the feeding position $d$ are varied to fine tune the CP characteristics of the antenna. The loops are placed at the aperture of the dielectric-loaded cavity and are electromagnetically coupled with a feeding line that is located on the same

**TABLE 1 Optimized Values of the Proposed Antenna**

| Parameters | Value (mm) |
|---|---|
| $G$ | 86.6 |
| $H$ | 7.85 |
| $w_c$ | 66.6 |
| $h_c$ | 17.9 |
| $L$ | 34.0 |
| $w_1$ | 1.3 |
| $w_2$ | 2.8 |
| $w_g$ | 1.6 |
| $T$ | 11.8 |
| $D$ | 25.05 |
| $l_f$ | 33.2 |
| $w_f$ | 26.9 |

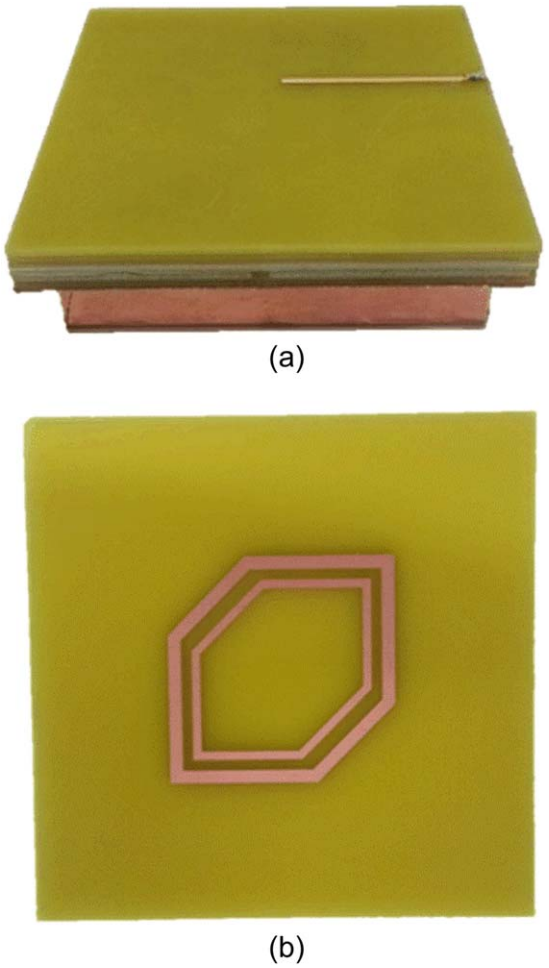


**Figure 2** Fabricated antenna. (a) Fabricated antenna. (b) Resonant loops. [Color figure can be viewed in the online issue, which is available at wileyonlinelibrary.com]

substrate material at a distance of $h$. The feeding line is designed as a microstrip line with a length of $l_f$ and a width of $w_f$, and its length is determined to be about a half wavelength in the GPS L1 band.

The proposed antenna is then optimized to further improve the impedance matching and radiation characteristics using a genetic algorithm (GA) in conjunction with the FEKO EM simulator [10,11], and optimized values are listed in Table 1. To demonstrate the suitability of the proposed antenna, we fabricate the antenna structure, as shown in Figure 2(a), and Figure 2(b) shows the photograph of the fabricated polygon loops placed between the feeding line and the dielectric-loaded cavity.

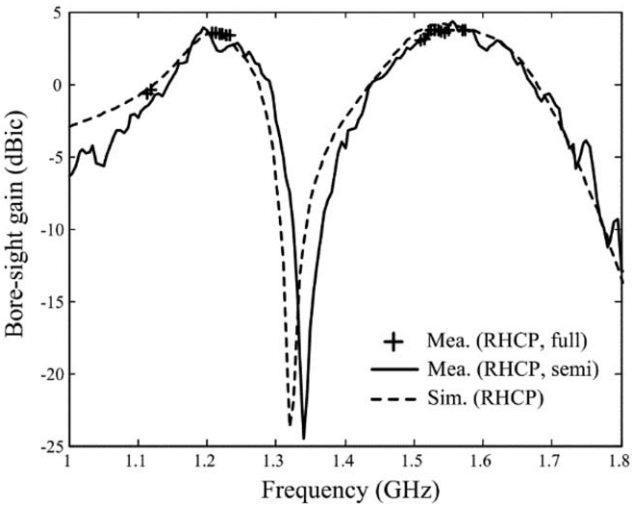


**Figure 4** Bore-sight gain of the proposed antenna

## 3. MEASUREMENT AND ANALYSIS

Reflection coefficients are measured in a semi-anechoic chamber and radiation characteristics, such as bore-sight gain, axial ratio (AR), and radiation patterns, are measured in a full-anechoic chamber. Figure 3 shows the comparison of the measured and simulated reflection coefficients as a function of frequency. The measured values at 1.5754 and 1.2276 GHz are −10.4 and −12.8 dB, respectively; these values are in good agreement with the simulated values of −11.8 and −13.6 dB. In addition, the fractional 10 dB bandwidth is 10 MHz for both the measurement and the simulation, and the values are 8.3% (1.48–1.61 GHz) and 8.1% (1.20–1.30 GHz) for the two frequency bands.

Figure 4 shows the comparison of measured and simulated bore-sight gains. The dashed line indicates the simulated data, and the measured values obtained are indicated by "+" symbols. We

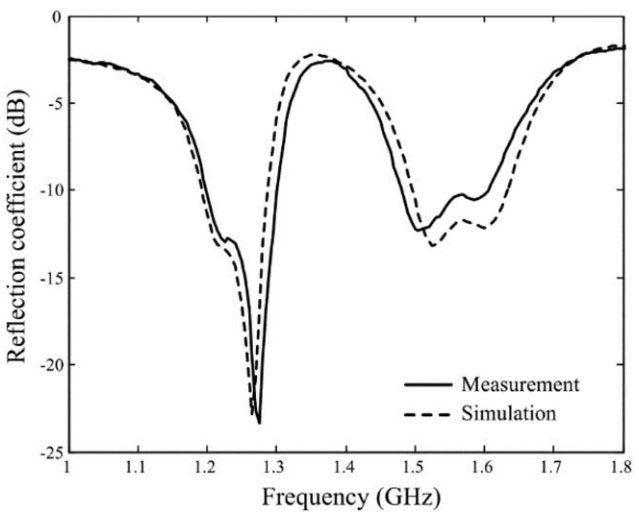


**Figure 3** Reflection coefficients of the proposed antenna

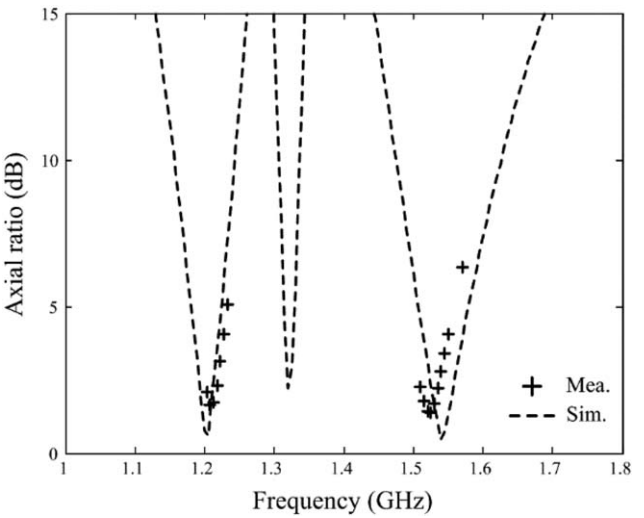


**Figure 5** Axial ratio of the proposed antenna

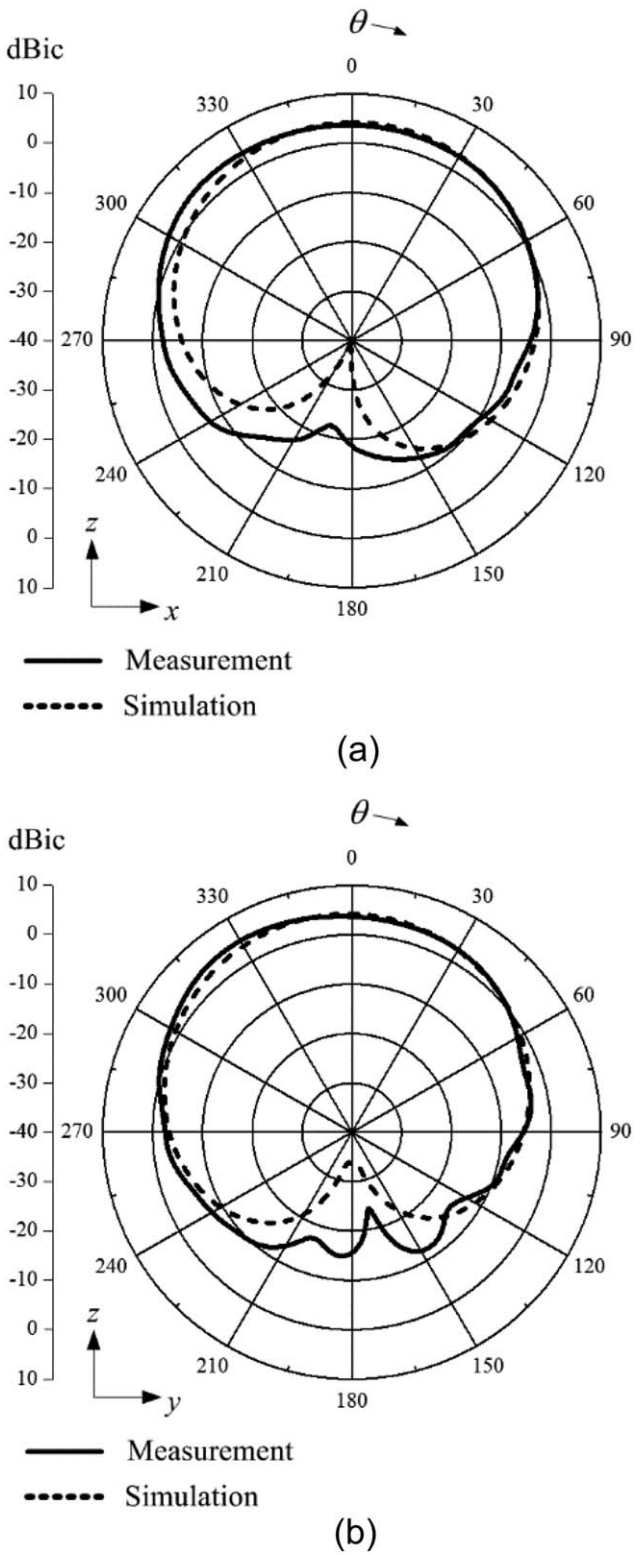


**Figure 6** 2-D patterns of the proposed antenna (1.5754 GHz). (a) *z–x* plane. (b) *z–y* plane

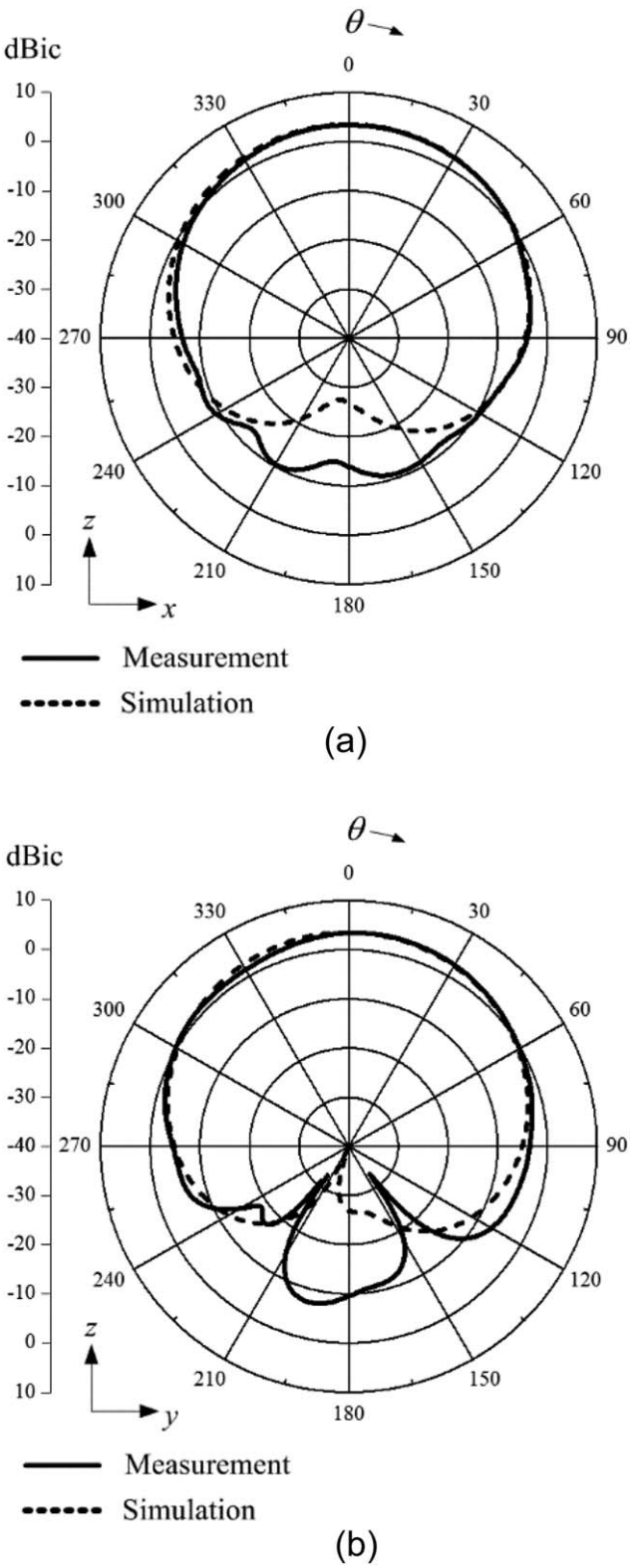


**Figure 7** 2-D patterns of the proposed antenna (1.2276 GHz). (a) *z–x* plane. (b) *z–y* plane

also present the measured results with the solid line to provide a continuous curve according to the frequency. The measured gain values are 3.7 and 3.4 dBic at 1.5754 and 1.2276 GHz, respectively; these values indicate that the antenna maintains high directivity in the bore-sight direction due to its cavity structure.

Figure 5 provides the comparison between the measured and simulated AR of the antenna. The antenna shows the minimum AR values of 1.4 dB at 1.525 GHz and 1.7 dB at 1.208 GHz, and its 3 dB AR bandwidths are 42 MHz (1.563–1.521 GHz) and 26 MHz (1.190–1.216 GHz).

Figures 6(a) and 6(b) show the comparisons of the measured and simulated radiation patterns in the *z–x* and *z–y* planes at 1.5754 GHz. The half-power beam width (HPBW) of the antenna

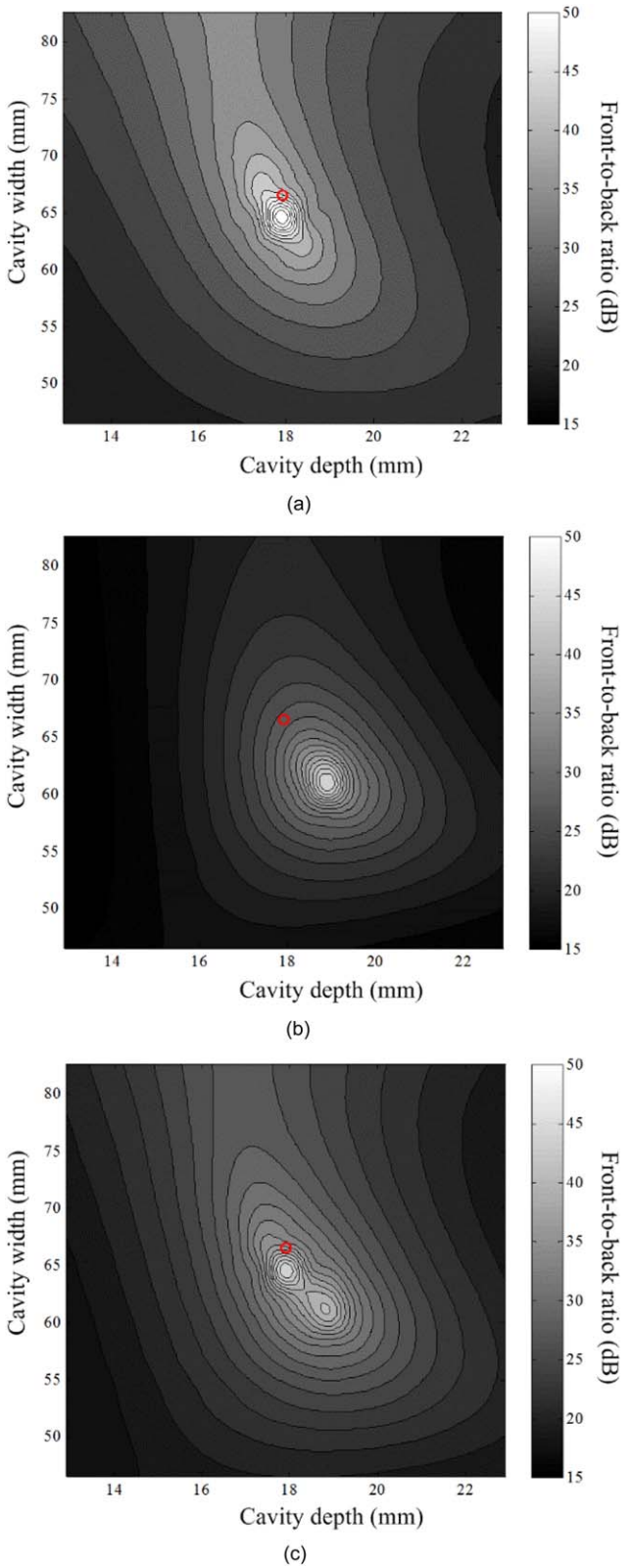


**Figure 8** Contour plot of the front-to-back ratio. (a) 1.5754 GHz. (b) 1.2276 GHz. (c) Average FBR. [Color figure can be viewed in the online issue, which is available at wileyonlinelibrary.com]

is 120° in the $z$–$x$ plane and 118° in the $z$–$y$ plane, and the average FBR of the two planes is 22.4 dB. Figures 7(a) and 7(b) illustrate the same 2-D patterns at 1.2276 GHz with an average FBR of 15.6 dB, and their HPBWs are 103° and 105°. Although the FBR is slightly decreased in the lower frequency band due to the smaller electrical size of the cavity, it still has higher FBR values in the two frequency bands compared to that in the air-filled cavity [9].

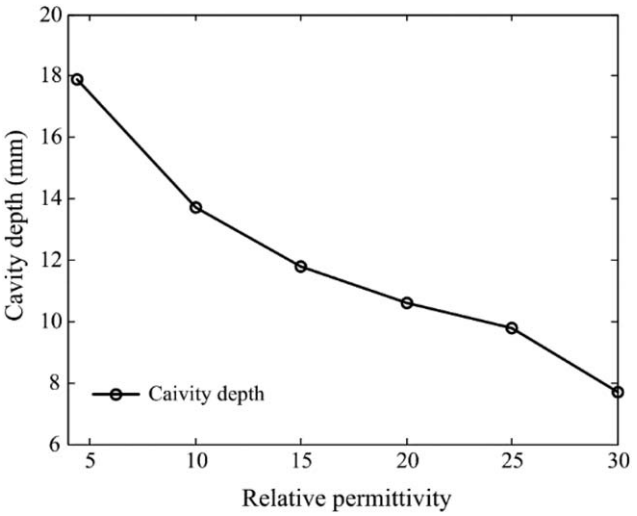


**Figure 9** Relative permittivity vs cavity depth

To analyze the effects of the cavity width and depth, we vary the width from 46.6 to 82.6 mm at intervals of 2 mm and vary the depth from 12.9 to 22.9 mm at intervals of 0.5 mm. The horizontal and vertical axes indicate the range of the width and depth, respectively, and the average FBR values in the two frequency bands are specified by contours for each cavity dimension, as shown in Figures 8(a) and 8(b). The optimized cavity dimension is indicated by a circular marker at each figure, and the average FBR in the two frequency bands is illustrated in Figure 8(c). As can be seen, the FBR is maximized to 60.8 dB when $w_c = 64.6$ mm and $h_c = 17.9$ mm at 1.5754 GHz, and the peak FBR at 1.2276 GHz is 44.7 dB when $w_c = 60.6$ mm and $h_c = 18.9$ mm.

Figure 9 shows the variation of the optimum depths for the dielectric-loaded cavity according to various dielectric constants. The horizontal axis indicates the dielectric constant of the cavity material, which is varied to 4.4, 10, 15, 20, 25, and 30. The vertical axis represents the optimum cavity depth that maximizes the FBR averaged in the two frequency bands, and each data point of the solid line is separately obtained from the same GA process introduced in Section . We can verify that the cavity depth is miniaturized up to 7.7 mm with an average FBR of 26 dB when the relative permittivity is increased to 30. This result demonstrates that the cavity size of the proposed antenna can be reduced without a significant degradation on the average FBR.

## 4. CONCLUSION

We have proposed the dual-band GPS antenna using the high-permittivity dielectric-loaded cavity. The antenna was fabricated, and its antenna characteristics were measured in a full-anechoic chamber. The results demonstrated that the dielectric-loaded cavity structure is suitable for increasing the directivity with measured bore-sight gains of 3.4 and 3.7 dBic with measured FBRs of 22.4 and 15.6 dB at 1.2276 and 1.5754 GHz, respectively. To analyze the effect of the dielectric constant to the cavity dimensions, we varied the dielectric constant from 4.4 to 30 and observed that the optimum cavity depth can be reduced as the value of the relative permittivity increases.

## ACKNOWLEDGMENT

This research was supported by Civil Military Technology Cooperation (CMTC) and the Basic Science Research Program through the National Research Foundation of Korea (NRF) funded by the Ministry of Education (No. 2015R1A6A1A03031833).

## REFERENCES

1. M. Epstein, The effects of polarization rotation and phase delay with frequency on ion spherically propagated signals, IEEE Trans Antenna Propag AP16 (1968), 548–553.
2. Z. Tu, D. F. Zhou, G. Q. Zhang, F. Xing, X. Lei, and D. W. Zhang, A wideband cavity-backed elliptical printed dipole antenna with enhanced radiation patterns, IEEE Antennas Wireless Propag Lett 12 (2012), 1610–1613.
3. I. K. Kim, N. Kidera, S. Pinel, J. Papapolymerou, J. G. Yook, and M. M. Tentzeris, Linear tapered cavity-backed slot antenna for millimeter-wave LTCC modules, IEEE Antennas Wireless Propag Lett 5 (2006), 175–178.
4. S. K. Hirasawa and Z. N. Chen, Circularly polarized rectangularly bent slot antennas backed by a rectangular cavity, IEEE Trans Antenna Propag 49 (2001), 1517–1524.
5. Q. Li and Z. Shen, An inverted microstrip-fed cavity-backed slot antenna for circular polarization, IEEE Antennas Wireless Propag Lett 1 (2002), 190–192.
6. W. Yang and J. Zhou, Wideband circularly polarized cavity-backed aperture antenna with a parasitic square patch, IEEE Antennas Wireless Propag Lett 12 (2013), 1610–1613.
7. K. F. Hung and Y. C. Lin, Novel broadband circularly polarized cavity-backed aperture antennas with traveling wave excitation, IEEE Trans Antenna Propag 55 (2007), 2382–2385.
8. C. Fumeaux, D. Baumann, and R. Vahldieck, Finite-volume time-domain analysis of a cavity-backed Archimedean spiral antenna, IEEE Trans Antenna Propag 54 (2006), 844–851.
9. W. T. Hsieh, T. H. Chang, and J. F. Kiang, Dual-band circularly polarized cavity-backed annular slot antenna for GPS receiver, IEEE Trans Antenna Propag 60 (2012), 2076–2080.
10. FEKO Suite 7.0, EM software and Systems, 2013, Available at: http://www.feko.info.
11. Y. Rahmat-Samii and E. Michielssen, Electromagnetic optimization by genetic algorithms, Wiley, New York, 1999.



# A NEW PROPOSAL TO CONVERTNEAR-FIELD INTO FAR-FIELD FOR PARABOLIC REFLECTORS

**J. Sosa Pedroza, M. Enciso Aguilar, S. Peña Ruiz, A. Rodríguez Sánchez, and E. Garduño Nolasco**
Unidad Profesional Adolfo López Mateos, Escuela Superior de Ingeniería Mecánica y Eléctrica, Instituto Politécnico Nacional, Edificio Z-4, 3er. Piso, Colonia Lindavista, Mexico, DF, 07738, Mexico; Corresponding author: edson.gn@live.com

*Received 20 November 2015*

**ABSTRACT:** *A modeling of a 1.5-m diameter parabolic reflector using the discrete Pocklington equation working at a frequency of 2.45 GHz has been presented; the proposal allows to obtain far-field radiation pattern from the reflected field close to the surface plate which has been first modeled in CST MWS and then it was converted into a current vector using the discrete Pocklington equation. Finally, the far-field pattern using antennas array theory was obtained. To validate the results, they compared them with the measurements of a real parabolic reflector.* © 2016 Wiley Periodicals, Inc. Microwave Opt Technol Lett 58:1595–1599, 2016; View this article online at wileyonlinelibrary.com. DOI 10.1002/mop.29862

**Key words:** *current distribution; far-field; near-field; parabolic reflector antennas; Pocklington equation*

## 1. INTRODUCTION

After 70 years of define behavior of antennas using analytical methods, nowadays the analysis became easier than before due the actual available numerical methods for electromagnetic analysis and antenna modeling, such as Method of Moments (MoM) [1], and others used in commercial software as Computer Simulation Technology (CST) whose performance is based on the Finite Integral Technique (FIT) [2]. Pocklington equation is also used for antenna analysis which solution is obtained thru MoM; Pocklington equation is an integral which is solved using MoM, but we have changed it into a discrete equation, to define virtual currents, after measurement or calculation of field in the conductor surface. Method of moments supposes that near the conductor are point sources which could be used in array theory to obtain far-field. We applied the method, presented in this article, to obtain the far-field radiation pattern of a parabolic reflector from the electric field on its surface (Rayleigh region).

Far-field is defined in the literature as the Fraunhofer region [3], depending of antenna dimensions as Eq. (1) shows.

$$d = \frac{2L^2}{\lambda} \tag{1}$$

where, $L$ is the largest antenna dimension and $\lambda$ is the wavelength.

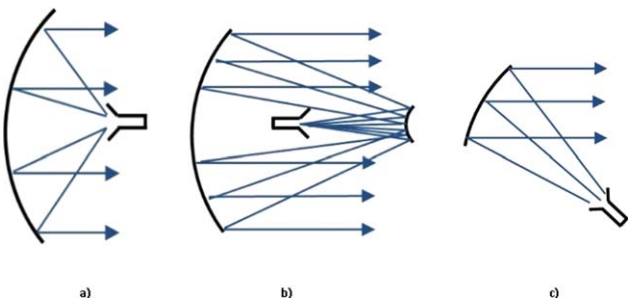


**Figure 1** Types of reflector (**a**) parabolic, (**b**) Cassegrain, and (**c**) asymmetric. [Color figure can be viewed in the online issue, which is available at wileyonlinelibrary.com]

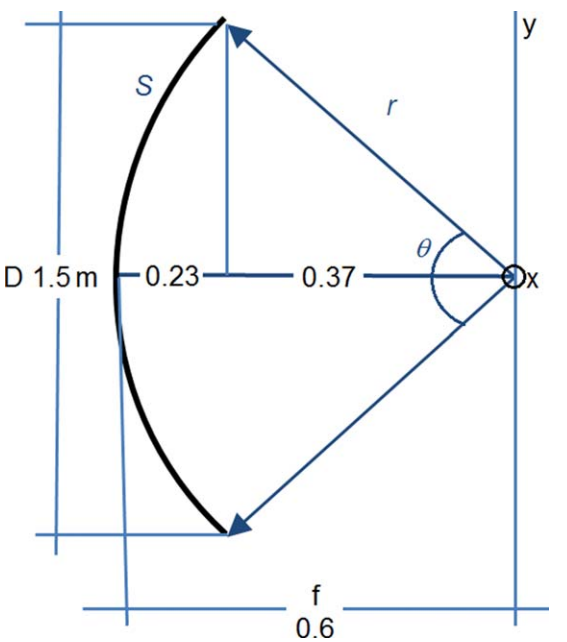


**Figure 2** Paraboloid reflector geometry. [Color figure can be viewed in the online issue, which is available at wileyonlinelibrary.com]